Chaos, Solitons & Fractals: X 11 (2023) 100099

Contents lists available at ScienceDirect

Chaos, Solitons & Fractals: X

journal homepage: www.elsevier.com/locate/csfx

Public goods games played on hypergraphs, by agents with bounded learning and planning

Prakhar Godara *, Stephan Herminghaus

Max Planck Institute for Dynamics and Self-Organization, Am Fassberg 17, Goettingen, 37077, Germany

A B S T R A C T

Public goods games between model agents with bounded rationality and a simple learning rule, which have been previously shown to represent experimentally observed human playing behavior, are studied by direct simulation on various lattices with different network topology. Despite strong coupling between playing groups, we find that average investments do not significantly depend upon network topology, but are determined solely by immediate local network environment. Furthermore, the dependence of investments on characteristic agent parameters factorizes into a function of individual cognitive budget, K, and a simple function $1/(1+c(0)/\beta)$, where $c(0)$ is the group centrality and $\beta = 12.5$ for all networks investigated. Given the good agreement of agent behavior with available experiments, this seems to indicate that even complex societal networks of investment in public goods may be accessible to predictive simulation with limited effort.

1. Introduction

The sustainable management of the ecological niche of humankind on planet Earth is increasingly being recognized as a sizeable problem, attracting growing interest of scientific research across disciplines [1–3]. Aside from limited planet resources and rapidly changing climate conditions, a topic of major concern is the possible response of human societies to such stimuli [4,3,5]. In order to anticipate these responses, and to potentially advise policy makers to come up with appropriate legislatory precautions, a thorough understanding of the collective behavior of humans in dense societies needs to be achieved.

Given the complexity of the behavior even of a single human, this may seem entirely out of reach at first glance. However, it is well known that in systems consisting of sufficiently many similar entities in mutual interaction, quite precise predictions may be possible on collective phenomena, even if little is known about the individual entities. We can precisely predict, e.g., the critical exponents of all singular quantities of a condensed matter system close to a phase transition solely from the number of degrees of freedom of the order parameter and its dimensionality, without even knowing which molecules the system is composed of [6]. Similar statements hold even if none of the many constituents (i.e., molecules) are identical, as may be the case in polymers [7]. In fact, many similarities between phase transitions and collective phenomena in societies have been demonstrated [8–13]. Consequently, methods of statistical physics are meanwhile widely applied to social systems, with ever growing success [11,14,12,13]. The main challenge, and subject of lively debate [4,15,11,16–18,3,19,20,5], is to come up with model agents which are sufficiently simple to allow for large scale simulations, and at the same time model traits of human interaction behavior which are relevant for the respective study.

2. Public goods games

A well established, and much studied, paradigm of interaction of human agents in societies is the well-known public goods game (PGG). In its standard game-theoretic setting, the PGG is played among N players over a total of T periods, where T is known to all players. In each period $t \leq T$, each player i is given a fixed integer number, τ, of tokens, a fraction $f_{i,t} \in [0, \tau]$ of which they can invest anonymously into a public pot[1]. The immediate reward of the ith player in that period is given by

$$G_{i,t} = \alpha \sum_{j=1}^{N} f_{j,t} - f_{i,t} \tag{1}$$

* Corresponding author.
E-mail addresses: prakhar.godara@ds.mpg.de (P. Godara), stephan.herminghaus@ds.mpg.de (S. Herminghaus).

[1] τ thereby just provides a scale of coarse-graining of the investments. Following a widely followed convention in the field [21,20], and without loss of generality, we use $\tau = 20$ throughout this article.

https://doi.org/10.1016/j.csfx.2023.100099
Received 8 March 2023; Accepted 21 July 2023
Available online 8 August 2023

where α is multiplying factor which is known to all players.[2] This can be written as

$$G_{i,t} = \alpha(N-1)\mu_{i,t} - (1-\alpha)f_{i,t}, \tag{2}$$

where $\mu_{i,t} = \frac{\sum_{k\neq i} f_{k,t}}{N-1}$ is the average contribution of other players. The total gain for the ith player can then be defined as $G_i = \sum_t^T G_{i,t}$.

This game may be taken as a model of a vast number of real situations of human interaction. In a shared household, participants fulfill chores as an investment (f_i) into a pleasant atmosphere as the common good (G), members of a sports club invest donations (f_i) for enjoying common goods such as a well-maintained playing court (G), members of an association invest personal commitment (f_i) in the common good of a thriving association (G), and so on. A substantial fraction of societal interaction can, in this paradigm, be viewed as an enormously complex network of PGG, which interact through agents participating in several PGG simultaneously. Judging from the mentioned analogies to condensed matter systems, one might anticipate that the topology of this network has a major impact upon the collective investment behavior of the agents.

Eq. (2) describes the gain for a given player playing in one period, in one group. In a network of interacting PGG groups, the corresponding gain becomes the sum of gains over all groups the agent plays in. Notice that the gains in each of these groups are independent. Therefore, in order to find a favorable policy in a particular group, each agent needs to keep in mind the actions of other players in that group alone. The dynamical interaction between groups comes about through the learning of the agents, i.e., their gradually updating their internal model of other player's behavior. We assume that each agent bears one such model for players in general, i.e., for the players of all groups it is playing in.

The PGG networks modeling a society are very complex as compared to the networks of nearest-neighbor interaction in a condensed matter system. In the latter, interactions are all of one kind (or a few) and extend over a set of spatially nearest (perhaps including next nearest) neighbors. Coordination numbers (i.e., network degrees) are small and homogeneous, and the topology of the network is strictly determined by the dimensionality. In contrast, the number of games agents participate in may vary strongly, and the topology of the network of interactions between groups, the size of which may also vary vastly, does not need to bear any relation to a network of proximity in a space of fixed (integer) dimensions. Hence one must be prepared to find qualitative differences to collective behavior in condensed matter systems when simulating complex networks of PGG, and universality classes as in phase transitions may not hold. As we will show, the investment behavior of agents can most probably be anticipated solely on the basis of rather local network descriptors, and network topology is found to be surprisingly irrelevant.

2.1. PGG agents

We employ model agents we have developed before [20,22], guided by progress in intelligence research [23,24]. While it has been claimed that reinforcement learning is *the* essential ingredient of agents reproducing experimentally observed PGG playing behavior [25,18], we could show that agents with bounded rational foresight with no learning capabilities at all may provide an even better account of experimental data [21,20]. Not only do they quantitatively reproduce the commonly observed downward trend of average investments during a game, they are also capable of accounting for the substantial period-to-period variance of these investments [21]. When bestowing a simple learning mechanism to these agents, as appears plausible for long-time playing settings, we furthermore obtained complex dependencies of average investment upon group size [22], as had been observed in a number of real-world settings [26,27]. The resulting model agent is still sufficiently simple to be used in large scale simulations such as those needed to investigate collective behavior in complex PGG networks.

Consequently, in the present paper we consider bounded learning and planning agents as described before [20,22], playing a spatially extended PGG (SPGG). The agent model is composed of two parts - *learning* and *planning*. Learning refers to agents observing the past game behavior of other agents in order to make a predictive model of them, while planning refers to making use of this model to chart out an optimal course of action in a particular game. In the following we describe the learning and planning mechanisms of an agent in a single group.

2.2. Planning mechanism

To describe the planning mechanism, we assume that agent i has a predictive model of other agents incorporated as a transition function,

$$Q(\mu_{i,t}|\mu_{i,t-1}, f_{i,t-1}) = g(\mu_{i,t}; p, \sigma). \tag{3}$$

It describes the likelihood of other agents' next action (expressed by $\mu_{i,t}$), given the previous state of the game $(\mu_{i,t-1}, f_{i,t-1})$. $g(\mu; p, \sigma)$ is the truncated Gaussian distribution on the interval $[0, \tau]$, where σ is the variance of the distribution, which we fix to $\sigma = 3$ throughout the article. $p(\mu_{i,t-1}, f_{i,t-1})$ is the peak position of the distribution as given by

$$p = \begin{cases} \mu_{i,t-1} + \xi_+^i|\mu_{i,t-1} - f_{i,t-1}|, & \mu_{i,t-1} - f_{i,t-1} < 0 \\ \mu_{i,t-1} - \xi_-^i|\mu_{i,t-1} - f_{i,t-1}|, & \mu_{i,t-1} - f_{i,t-1} > 0, \end{cases} \tag{4}$$

where ξ_+^i and ξ_-^i parameterize Q. As the ith agent can influence the actions of others solely through its contributions (because players play anonymously and do not interact otherwise), the parameters ξ_+^i and ξ_-^i describe to which degree agent i believes to be able to encourage or discourage other agents to contribute. In that sense, $\xi_\pm^i$ is the model the agent has of the other agents. As far as planning is concerned, we do not bother about how the agent comes up with a particular set of values $\xi_\pm^i$, but rather what decisions does the agent come up with, given Q.

Let us assume that the agent has a policy of its own actions from period t until the end of the game (period T) given by $P(f_t^T) = \prod_{t'=t}^T P(f_{i,t'}|\mu_{i,t'-1})$. By making use of Q and $P(f_t^T)$ one can write the path probabilities of various game trajectories. Combining it with the gain of the agent associated with a trajectory, one can write down the expected utility for the policy as a path integral. This expected utility can then be maximized to find the optimal policy. Finally, the path integral maximization can be written in a recursive form, described by a Bellman equation [28] given by

$$V_t^* = \max_{P(f_t^T)} \sum_{f_{i,t},\mu_{i,t}} P(f_{i,t}|\mu_{i,t-1}) \Big[Q \cdot G_{i,t}(f_{i,t}, \mu_{i,t}) + \gamma Q \cdot V_{t+1} \Big], \tag{5}$$

where * is to indicate a maximized quantity. $\gamma \in [0, 1]$ represents a foresight which exponentially 'decays' into the future, discounting for future rewards. If we also include bounds on the computational capabilities of the agent [20], an additional term appears in Eq. (5), which then becomes

$$V_t^* = \max_{P(f_t^T)} \sum_{f_{i,t},\mu_{i,t}} P(f_{i,t}|\mu_{i,t-1}) \Big[Q \cdot G_{i,t}(f_{i,t}, \mu_{i,t}) - \frac{1}{\beta} \log \frac{P(f_{i,t}|\mu_{i,t-1})}{P_0(f_{i,t}|\mu_{i,t-1})} + \gamma Q \cdot V_{t+1} \Big]. \tag{6}$$

The Lagrange parameter β comes about from the additional constraint $\frac{1}{\beta}\left(D_{KL}\left(P^*(f_{i,t}|\mu_{i,t-1})||P_0(f_{i,t}|\mu_{i,t-1})\right) - K\right) = 0$, where K is the computational budget of the agent. Essentially, the additional term penalizes

[2] It can be seen from Eq. (1) that the game has very trivial optimal strategies for $\alpha \geq 1$ (contribute everything) or $\alpha \leq \frac{1}{N}$ (contribute nothing) and therefore the only "interesting" case where the personal and collective gains conflict and give rise to a social dilemma is the case when $\frac{1}{N} < \alpha < 1$. Outside this range, α does not have much qualitative impact on game dynamics. Therefore we set $\alpha = 0.4$ throughout this article, which is a value commonly found in literature.

high Kullback-Leibler (KL) divergence of the posterior (P) and the prior (P_0) policies, for some given P_0 for the agent. The solution of the optimization problem in Eq. (6) then provides us with the bounded optimal policy $P(f_t^T) = \prod_{t'=t}^{T} P(f_{i,t'}|\mu_{i,t'-1})$.

In conclusion, in period t, given a model $\xi_{\pm}^i$, a prior policy P_0, a computational budget K and exponentially decaying foresight γ that describe agent i's properties, the agent makes use of Eq. (6) to evaluate the best policy. Now we concern ourselves with how the agent comes up with its model of other agents i.e. $\xi_{\pm}^i$.

2.3. Learning mechanism

Following [22] we consider the learning mechanism as a maximum likelihood estimation over the transitions observed by the agent. The task of learning for agent i in period t then is the task of finding the tuple $\xi_{\pm}^i$ that is most representative of the state transitions observed by the agent. This can be written as

$$\xi_{\pm}^{i\,*}(t) = \arg\max_{\xi_{\pm}^i(t)} \left[\sum_{w=t-1}^{2} \gamma_p^{t-w} \log Q(\mu_{i,w}|\mu_{i,w-1}, f_{i,w-1}) - (1-\gamma_p)(\xi_{\pm}^i(t) - \xi_{\pm}^i(t-1))^2 \right]. \tag{7}$$

The summation is over all observed past and the summand is the weighted log likelihood of having observed a particular transition from period $w-1$ to period w. The exponential weighting factor γ_p represents the recency bias or the bounded memory of the agent [29] as it weights recent transitions more than earlier transitions. Finally the last summand represents the tendency of the agent to not update its model. Therefore when $\gamma_p = 0$ the agent performs no learning and maintains its previously believed model, and when $\gamma_p = 1$ the agent looks arbitrarily back in the past and performs the maximum likelihood estimation and updates its model.

As we are interested in collective effects here, we allow all players to play in multiple groups simultaneously. Their rewards in single playing groups are evaluated independently and then summed over all groups they play in. In this setting, beyond just the intra-group dynamics, the network of connections between groups and players also becomes of relevance through the fact that players play in several groups.

3. PGG networks

The interaction structure for players playing multiple PGGs simultaneously with different groups of players is best captured by *hypergraphs*. In what follows, we give a brief account of the concept hypergraphs, and how connects to our system of interest. We will then describe how to adapt the behavioral dynamics, as described for single groups in the previous section, to the spatially extended setting of an SPGG.

3.1. Hypergraphs

A hypergraph [30] is a graph whose edges are allowed to connect more than two nodes. An edge in a hypergraph is called a *hyperedge*. Hence a hypergraph $\mathcal{H}$ can be defined as a tuple $\mathcal{H} = (V, E)$, where V is a finite set of nodes v_i indexed by $i \in \{1, \dots, |V|\}$ and E is a finite set of hyperedges e_j indexed by $j \in \{1, \dots, |E|\}$, where each hyperedge is a non-empty subset of V. One can completely specify a hypergraph by an *incidence matrix* H_{ij} where $i \in \{1, \dots, |V|\}$ and $j \in \{1, \dots, |E|\}$ and

$$H_{ij} = \begin{cases} 1 & v_i \in e_j, \\ 0 & \text{else.} \end{cases} \tag{8}$$

In this work, we identify the nodes in $\mathcal{H}$ as the agents and the edges are identified as the various groups the agents play in. As most literature on PGG considers four player games, in this work we consider agents playing on 4-*regular* hypergraphs,[3] but each agent is allowed to play in arbitrarily many groups. Other than this we consider no restrictions on the topology of the hypergraphs.

3.2. Agent dynamics on hypergraphs

Now that we have introduced the interaction structure, our task remains to adapt the agent behavioral dynamics from Sec. 2 to the spatially extended setting. Let us consider an SPGG being played on a hypergraph $\mathcal{H}$ with $|V| = N_p$ players and $|E| = N_g$ groups. In order to carry out the discussion on the agent model we describe it from the perspective of an arbitrary agent given by an index $i \le N_p$, which plays in $k \le N_g$ different groups given by the indices $i_1, \dots, i_k$.

As already mentioned, agent i plans in each of the k groups independently. This means that agent i in period t, makes use of Eq. (6) to find the optimal policy for itself and then, for each group it plays in, it independently samples an investment from the conditional distribution $P(f_{i,t}|\mu_{i,t-1})$ by conditioning on the observed $\mu_{i,t-1}$ of that group.

Learning, on the other hand, is not done independently in each group. Essentially, the exponentially weighted log likelihood in Eq. (7) is summed not only over all observed past of one group, but over all groups. By suitably modifying the notation to also include the group identity, one can write the analogous equation as

$$\xi_{\pm}^{i\,*}(t) = \arg\max_{\xi_{\pm}^i} \sum_{m=1}^{k} \left[\sum_{w=t-1}^{2} \left(\gamma_p^{t-w} \log Q(\mu_{i,i_m,w}|\mu_{i,i_m,w-1}, f_{i,i_m,w-1}) \right) - (1-\gamma_p)(\xi_{\pm}^i(t) - \xi_{\pm}^i(t-1))^2 \right], \tag{9}$$

where the subscript i_m denotes that the quantity is being evaluated in group i_m with $m \le k$.

The learning and planning mechanisms can be then combined into a single agent which is defined by a quadruple of parameters, (m, K, γ, γ_p), where m parameterizes the prior policy of the agent.[4] In each round $t \in \{2, 3, \dots T\}$, the agent

1. **plans**: by considering the game state at $t-1$ in all the k groups it plays in and $\xi_{\pm}^i(t-1)$, the agent making use of Eq. (6) finds the best policy for itself.
2. **acts**: by sampling an investment, $f_{i,i_m,t}$, from the evaluated policy, after conditioning on the observed $\mu_{i,i_m,t-1}$ of each group $m \in \{1, \cdots, k\}$.
3. **learns**: after observing the state of the game in the current period t in all the k groups the agent learns and updates its model of the players by evaluating $\xi_{\pm}^i(t)$ from Eq. (9).

In period $t = 1$ the investments of the agent are sampled from its prior distribution $P_0(f_{i,1})$ for all the groups it plays in. In period $t = 2$ there is certainly planning based on observed behavior, but there is no learning, as the agent has not yet observed a transition.

4. Topology and dynamics

In our previous studies [20,22] we focused on how agent characteristics (m, K, γ, γ_p) impact the behavioral dynamics in PGG. Here we have, as an additional feature, namely, the interaction structure imposed by the hypergraph. It is then natural to investigate the specific impact of the interaction network structure on the agent dynamics, and thereby on possible collective phenomena in the system. This will be the main

[3] A k-regular hypergraph H is a hypergraph such that $|e_i| = k$ for all $i \in \{1, \dots, |E|\}$.

[4] We assume that the prior policy of the agent is given by the same distribution $P_0(f_{i,t})$ in each period t and the distribution is a truncated Gaussian centered around m and a fixed variance $\sigma_m = 5$.

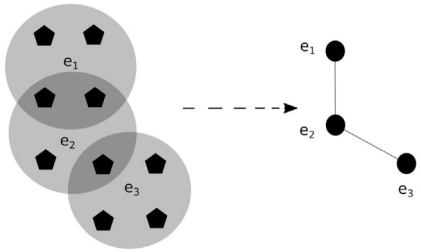

Fig. 1. Projecting a hypergraph to a line graph. The hyperedges (e_1, e_2, e_3) of the hypergraph correspond to the vertices of the line graph. Black pentagons correspond to agents, black circles correspond to groups.

question we pursue in the remainder of this article. Before we proceed, however, we need to clarify our concepts of "topology" and "dynamics", and to introduce the key descriptors of topology of the hypergraph as well as the relevant observables we will use to describe the agent behavioral dynamics.

4.1. Topological features

Hypergraphs (as opposed to graphs) provide the opportunity to consider two distinct types of interactions: inter-group and intra-group. While our previous studies have focused primarily on intra-group interactions, we focus here on inter-group interactions and their effect on contributions. The smallest unit of interest in this paradigm is a group. This allows us to project the uniform hypergraph to a corresponding *line graph* $\mathcal{L}$.[5] Fig. 1 shows a schematic of the projection of a hypergraph to the corresponding line graph. Notice that the hyperedges e_1, e_2, e_3 become vertices in the line graph and the information about the location of vertices of the hypergraph (black pentagons) gets lost when performing this projection. Therefore in a line graph all of the intra-group structure is lost and it remembers only non-zero overlaps between groups.

Our task now remains to choose the appropriate descriptor of the graph topology. Studying SPGG, we are interested in evaluating the degree of influence (measured through the dynamical observables) a particular group (i.e., a node in the line graph) has on other groups in the graph depending, e.g., on the distance between them. This is to determine how 'far' the influence of a group travels within the graph. Hence we need a suitable descriptor which represents the notion of a distance in a graph topology, and is suitable to quantify such propagation of influence.

A well-established class of such descriptors is the *Bonacich-Katz* class of centrality measures [31]. The Bonacich-Katz centrality of a node i in the line graph $\mathcal{L}$ is parameterized by two parameters ω, η and is given by

$$c_i(\omega, \eta) = \omega(I - \eta J)^{-1} J 1, \tag{10}$$

where I is the identity matrix, J is the adjacency matrix of $\mathcal{L}$ and 1 is a column vectors of all ones. Here ω is a constant multiplying factor and therefore doesn't impact the centrality ranking of the nodes and can therefore be ignored via an appropriate normalization. η parametrizes the expected radius of influence a particular group has on other groups, which is proportional to $(1-\eta)^{-1}$. It will be the main parameter of concern for us in this article. While for $\eta \to 0+$, c_i is equivalent to degree centrality and it corresponds to eigenvector centrality if $\eta \to \frac{1}{\lambda_{\max}} -$, where $\lambda_{\max}$ is the largest eigenvalue of the adjacency matrix of $\mathcal{L}$ [32].

[5] A line graph of a hypergraph $\mathcal{H} = (V, E)$ is a graph $\mathcal{L}(\mathcal{H}) = (V_\mathcal{L}, E_\mathcal{L})$, where $V_\mathcal{L} = E$ and two vertices e_i, e_j in are connected in $\mathcal{L}$ iff. $e_i \cap e_j \neq \emptyset$.

4.2. Dynamical features

In order to quantify cooperation in PGG, a natural observable of interest is the average contribution of the group or player. Let us consider an agent i where $i \leq N_p$. Let the set of groups the agent plays in be given by $p_i = \{k | H_{ik} \neq 0\}$. Then we define the average agent contribution as

$$A^{\text{agent}}_{i,t} = \frac{\sum_{j \in p_i} f_{i,j,t}}{|g_i|}, \tag{11}$$

and the corresponding ensemble averaged quantity given by $\langle A^{\text{agent}}_{i,t} \rangle$. The corresponding average group contribution for a group j where $j \leq N_g$ is defined as

$$A^{\text{group}}_{j,t} = \frac{\sum_{i \in g_j} f_{i,j,t}}{4}, \tag{12}$$

where $g_j = \{i | H_{ij} \neq 0\}$ and the ensemble average quantity is given by $\langle A^{\text{group}}_{j,t} \rangle$. For both these quantities the corresponding time average quantity is given by $A'_i = \frac{\sum_{t=0}^{T} A'_{i,t}}{T}$.

The above quantities are averaged over time, and therefore hold no information regarding the interactions between groups unfolding over time. The latter can be investigated by considering temporal correlations between group trajectories. To this end, we consider the correlation matrix C_{ij}, in which the i,j entry is the correlation between trajectories of groups i and j. It is given by

$$C_{i,j} = \frac{1}{T} \sum_{t=0}^{T} \frac{\sigma_{A^{\text{group}}_{i,t} A^{\text{group}}_{j,t}}}{\sigma_{A^{\text{group}}_{i,t}} \sigma_{A^{\text{group}}_{j,t}}}, \tag{13}$$

where σ_{XY} is the covariance of random variables X, Y given by $\langle XY \rangle - \langle X \rangle \langle Y \rangle$ and σ_X is the variance of X. Because the correlation between two group averaged trajectories is symmetric over the two groups, it is a natural measure for us as the coupling between groups which is mediated by the learning mechanism of the common player(s) also has no way to break the symmetry between the groups.

5. Results

As we intend to evaluate the specific impact of network topology on the dynamics, we will keep the agent characteristics homogeneous and consider heterogeneity only through graph topology. Therefore we consider identical agents that are embedded on a random hypergraph (for details on how these random hypergraphs are generated see App. A).

For these agents we fix $(m, \gamma) = (10, 0.9)$[6] and additionally, we consider $\gamma_p = 0.9$. This choice reflects the fact that in our model the interactions between neighboring groups are mediated by learning. Lower values of γ_p would weaken the group interactions, thereby rendering the network structure pointless. On the other hand for $\gamma_p \approx 1$ it is observed that something similar occurs for longer times [22], as every new observation has only a diminishing impact on the agents' preferences. As we will see in the following, even though we create a setup (choice of parameters) that qualitatively maximizes the group interactions, the resulting dynamics still seems mostly independent of the various topological features.

We consider ten randomly generated hypergraphs with $(N_p, N_g) = (64, 25)$ with all the agents described by $(m, \gamma, \gamma_p) = (10, 0.9, 0.9)$ and $K \in \{0, 1.5, 3, 4.5\}$. For each random hypergraph we perform the ensemble average of 5000 simulation runs. Following the question asked in the beginning of Sec. 4 we investigate, in a random hypergraph with all identical agents, what topological descriptor is the most appropriate to predict average group contribution. As already mentioned we consider the class of descriptors given by Bonacich-Katz centrality and we

[6] Both (m, γ) have only a trivial monotonic impact on average contribution (as shown in [20]) and therefore do not change the results of this article qualitatively.

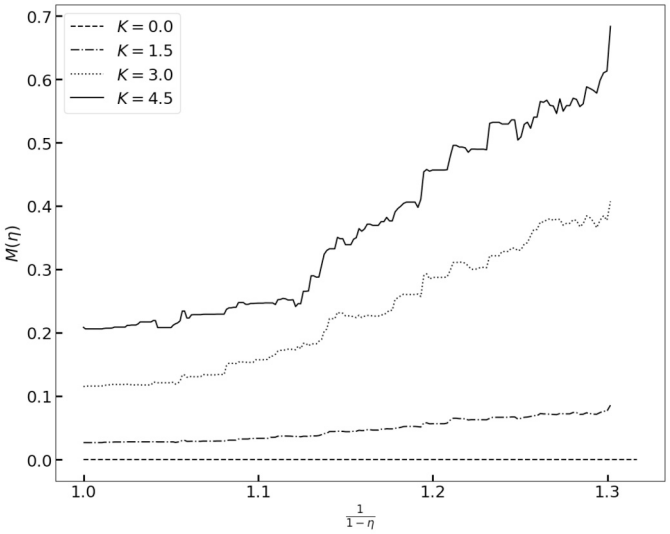

Fig. 2. Dependence of conditional expected contribution variance, $M(\eta)$, upon radial distance of influence, as expressed by $(1-\eta)^{-1}$. The curves are averaged over ten hypergraphs of size $(N_p, N_g) = (64, 25)$ for agents with $K = 0$ through $K = 4.5$.

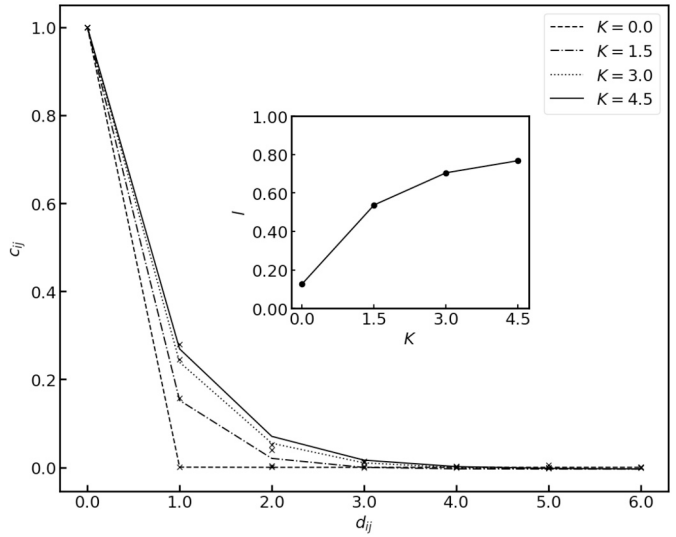

Fig. 3. Group trajectory correlations as a function of the shortest distance between the groups for groups of agents with $K = 0$ through $K = 4.5$. Crosses are data points, polygons are exponential fits.

consider the most "appropriate" centrality measure (or the most appropriate η) as the one that minimizes the function

$$M(\eta) = \int \theta_{\langle A_j^{\text{group}}\rangle|(c_j(\eta)=c)} dc. \tag{14}$$

Here the variance is defined as

$$\theta_{\langle A_j^{\text{group}}\rangle|(c_j(\eta)=c)} = \text{VAR}\{\langle A_j^{\text{group}}\rangle | c \le c_j \le c + dc\}, \tag{15}$$

for some choice of discretization. Essentially, every value of η is an assignment of a centrality to each node. We wish to find that assignment η such that given a centrality $c(\eta) = c_0$, the variance of the average contributions corresponding to the nodes with the centrality close to c_0 is minimal when integrated over all c_0. In other words we wish to find η for which the scatter of the scatter plot between $\langle A_j^{\text{group}}\rangle$ and $c_j(\eta)$ is minimal.

In Fig. 2 we plot $M(\eta)$ curve averaged over 10 different random hypergraphs as a function of η and one can see that the global minimum of $M(\eta)$ is given by $\eta \approx 0$ for various values of agent parameters given by $K \in \{0, 1.5, 3, 4.5\}$ thereby indicating that the centrality measure with very small values of η best predicts the group average contribution independent of K. Recalling the definition of Katz centrality, smaller values of η correspond to smaller radii of influence. This then seems to indicate that it is the local topological features (in this case, node centrality i.e. number of neighbors) that are the best predictors of average group contribution.

In the above analysis there is no "dynamics" as such, as we have only considered the distribution of $\langle A^{\text{group}}\rangle$ across nodes of varying centrality. Therefore any claims of groups have a smaller "radius of influence" could be misguided if the above result is considered in isolation. In order to create a more robust picture of the radius of influence of a group, we consider how quickly do inter-group correlations decay as a function of the shortest distance between the groups.

Therefore, we proceed by comparing the correlation matrix C with the distance matrix D[7] to evaluate how the correlations between group average trajectories scale with the shortest distance between the groups. In Fig. 3 one can see that the correlation between group average trajectories falls down exponentially with the (shortest) distance between the groups with correlation lengths $l < 1$ (as shown in the inset). Thereby meaning that substantial correlations of a group's behavior is only with its immediate neighbors. This further corroborates that group contributions in SPGG are mostly governed by local interactions.

The locality of interactions in SPGG is a good news for two major reasons. First and the more obvious reason is that locality simplifies the analysis of the system, thereby allowing for the possibility of developing simpler effective dynamics that replicate these observations. The second reason is that, if group contributions are mostly governed by local interactions (in this case group centrality $c(\eta = 0)$), then even if we have graphs with different global structures but similar local structures we should observe similar behavior. The latter would seem to indicate a universality (i.e. global topology independent) in cooperation behavior across a large set of networks.

Fig. 4 presents the impact of group centrality $(c(\eta = 0))$ on the group average contribution for different values of K, for ten randomly generated hypergraphs. Different symbols correspond to different hypergraphs. For each value of K, the results are found not to differ significantly for different hypergraphs. This demonstrates that topological features of the hypergraphs are irrelevant to this end. Cooperation levels of groups are predominantly determined by the number of neighbors of the group. Quite surprisingly, one does not even need to consider how many players are shared between two neighbor groups (recall that $c(0)$ is measured from the line graphs and not the hypergraphs).

6. Discussion

Another observation from Fig. 2 is that $M(\eta)$ monotonically increases with K, attaining a minimal value at $\eta = 0$ for all K investigated. Having a higher scatter for higher K would seem to indicate that agents with higher K accommodate their contributions to more details of topology rather than just the number of groups they play in.[8] This is a view that also gets supported by looking at the variation of correlation lengths with K. In the inset of Fig. 3, it can be seen that correlation lengths increase with K, thereby indicating that as K increases, more distant neighbors become relevant as compared to lower

[7] A distance matrix D for a graph $\mathcal{L} = (V, E)$ is a matrix of size $|V| \times |V|$ where the i, j entry $D_{i,j}$ is the length of the shortest path between node i and node j in $\mathcal{L}$.

[8] The other end of the extreme is the case of $K = 0$, where the agents disregard any topological or dynamical features and play according to independent samples from a stationary prior distribution.

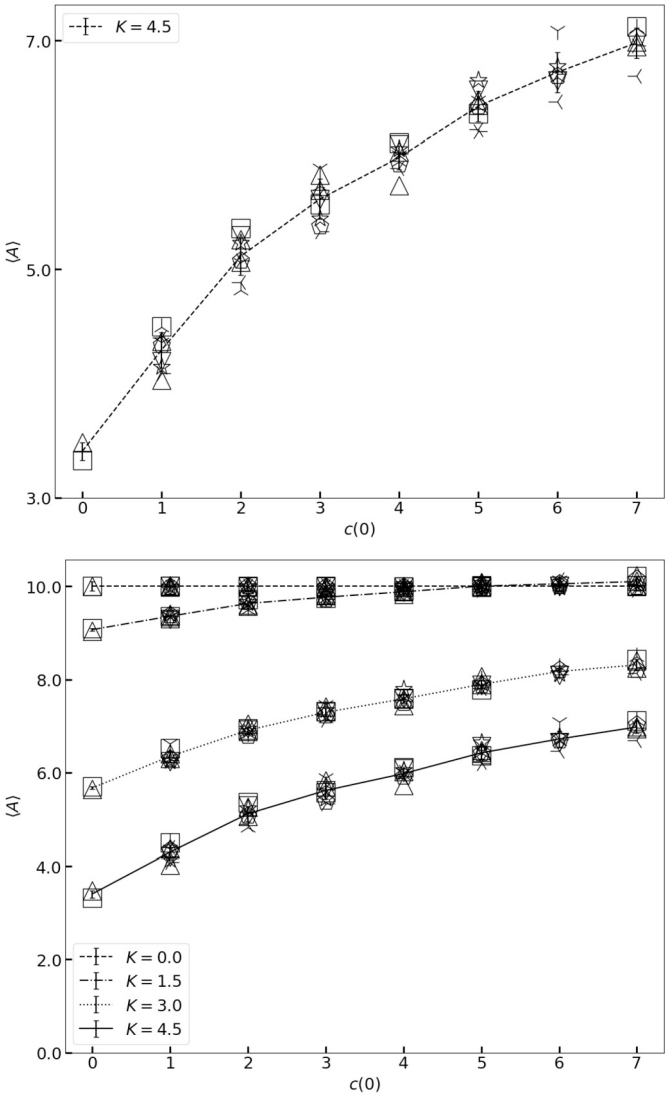

Fig. 4. Impact of group centrality on the group average contribution for ten randomly generated hypergraphs. Left panel: results for $K = 4.5$, with different symbols corresponding to different hypergraphs. Right panel: same as left panel for different values of K. Polygons connect averages over all hypergraphs, respectively.

values of K. Hence agents with higher values of K are more sensitive to the surrounding topology of the interaction network. However, the data suggest that the range of this sensitivity saturates at higher K, with the decay length staying below unity.

This sensitivity can also be seen in Fig. 4. Note that group centrality has a positive impact on group contributions irrespective of agent parameters, although agents with higher values of K experience an appreciably bigger increase in their contributions as compared to their lower K counterparts. In the following we quantify this sensitivity (to centrality) as a function of K.

We consider 3 different hypergraphs (their corresponding line graphs can be seen in Fig. 5), two of them generated randomly and one uniform square lattice, all with $(N_p, N_g) = (64, 25)$. We consider identical agents with K varying from 0.5 to 5 and average over 5000 simulation runs for each configuration (i.e. a pair of a value of K and one of the three hypergraphs). We then perform three-parameter fits on the average contribution curves with the ansatz,

$$A(c(0), K) = A_0(K) - \frac{h(K)}{1 + c(0)/\beta}. \tag{16}$$

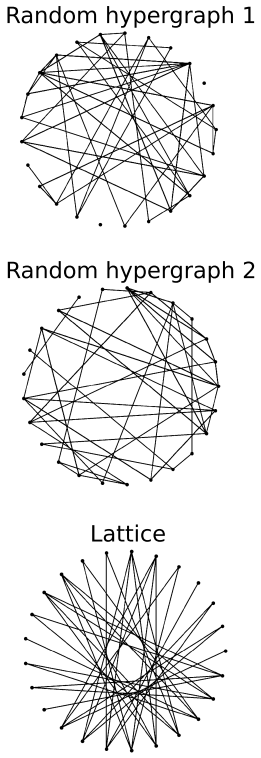

Fig. 5. Line graphs corresponding to three hypergraphs. Top two correspond to random hypergraphs and the bottom corresponds to square lattice.

As it turns out, A_0 does not vary appreciably with K.[9] Therefore we remove its dependence on K and treat it as a constant. Therefore, parameters A_0 and β are obtained by performing a fit on all configurations and h is fitted to each configuration separately. It turns out that setting $A_0 = 12.25$ and $\beta = 12.5$, the (fitted) values of $h(K)$ collapse onto a characteristic curve independent of the network topology. In Fig. 7 we plot three curves $h(K)$ for the corresponding hypergraphs as obtained from the fits. The empty symbols correspond to $(A_0 - A)/(1 + c(0)\beta)$ for each individual group, where A_0 and β take the aforementioned values. A and $c(0)$ for each group are obtained from the simulations. Within scatter, the data are well represented by eq. (16). In a similar fashion we also show the characteristic value of β to be well descriptive of the impact of group centrality (see Fig. 6). To conclude, the deviation from the 'trivial' case $K = 0$ seems to factorize as expressed by eq. (16), into a part depending on $c(0)$ and a function $h(K)$ which depends only on K. The latter starts off roughly linearly but saturates at higher values of K.

7. Conclusions

Based on previously developed model agents that boundedly learn and plan, we have explored collective behavior in SPGG on a variety of hypergraphs of different topology. What we find that collective investment behavior is determined essentially by local descriptors, with correlations decaying exponentially in space. Furthermore, the impact of local connectivity, $c(0)$, and rationality of the agent, K, on the expected average investment factorize in a universal way, independent of network topology. Its behavior can be quantified with a characteristic function as shown in Fig. 7 and lends itself to experimental test.

Finally, our work suggests that cooperation in SPGG can be driven by making the players more diverse i.e. increasing the number of groups

[9] Here we ignore the case of $K = 0$, as it represents a qualitatively trivial case, and the corresponding fitting procedure has non-unique global minima (both $h(0) \to 0$ and $\beta \to \infty$ lead to a flat curve).

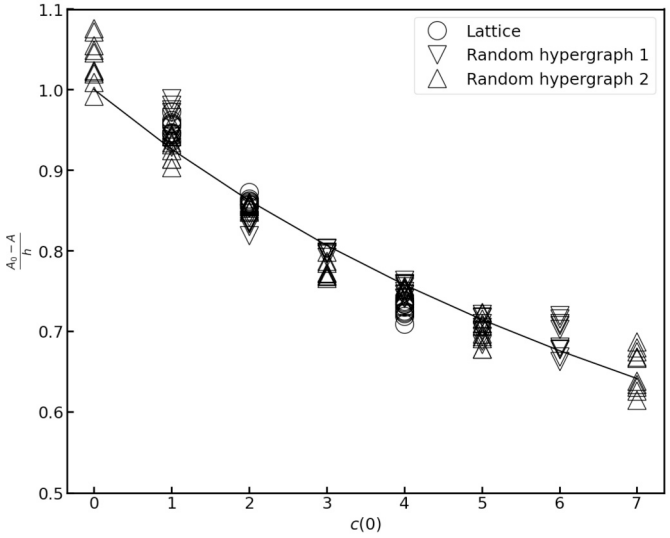

Fig. 6. $(A_0 - A)/h$ as a function of group centrality for the three hypergraphs. The corresponding data from the hypergraphs are represented by circles, triangle-up and triangle down. The solid line corresponds to the function $(1 + c(0)/\beta)^{-1}$ for $\beta = 12.5$.

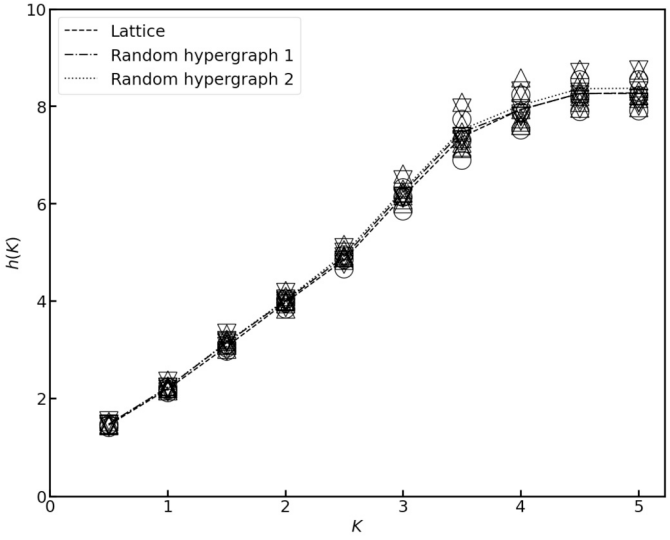

Fig. 7. $h(K)$ for three hypergraphs. Polygons (dashed, dash dotted and dotted) correspond to the best fit. The corresponding data from the hypergraphs are represented by circles, triangle-up and triangle down, respectively.

they play in and consequently increase inter-group connections. This observation is in line with results previously reported in [33], despite the fact that the authors follow a completely different modelling route.

Declaration of competing interest

The authors declare that they have no known competing financial interests or personal relationships that could have appeared to influence the work reported in this paper.

Data availability

The algorithms have been adequately described in the article. If someone still needs access to the codes, they can be made available on request.

Appendix A. Generating a random hypergraph

In Algorithm 1 we show our method of generating a random hypergraph. The function takes as input (N_p, N_g) and returns the incidence matrix for the hypergraph. It has to be kept in mind that $N_p \geq 4$ otherwise we will not be able to generate a 4-regular hypergraph and also $N_p \leq 4N_g$, because if $N_p > 4N_g$ there will be at least one player which doesn't play in any group, thereby effectively decreasing N_p until $N_p = 4N_g$.

Algorithm 1 Random hypergraph generation

```
function HYPERGRAPH(N_p, N_g)
    H = zeros(N_p, N_g)                          ▷ Incidence matrix
    for 1 ≤ i ≤ N_p do                           ▷ Each player gets a group
        filled = 0
        while filled = 0 do
            j = random (1, N_g)                  ▷ choose a random j ∈ [1, N_g]
            if Σ_k H_kj < 4 then
                H_ij ← 1
                filled ← 1
            end if
        end while
    end for
    for 1 ≤ j ≤ N_g do                           ▷ Each group gets 4 players
        while Σ_k H_kj < 4 do
            i = random(1, N_p)
            H_ij ← 1
        end while
    end for
    RETURN H
end function
```

References

[1] O'Neill DW, Fanning AL, Lamb WF, Steinberger JK. A good life for all within planetary boundaries. Nat Sustain 2018;1:88–95.
[2] Kotzé LJ, Kim RE. Earth system law: the juridical dimensions of Earth system. Earth Syst Gov 2019;1:100003.
[3] Alvarez-Rodriguez U, Battiston F, de Arruda GF, Moreno Y, Perc M, Latora V. Evolutionary dynamics of higher-order interactions in social networks. Nat Hum Behav 2021:1–10.
[4] Hauert C, Traulsen A, Brandt H, Nowak MA, Sigmund K. Via freedom to coercion: the emergence of costly punishment. Science 2007:1905–7.
[5] Winkelmann R, Donges JF, Smith KE, Milkoreit M, Eder C, Heitzig J, et al. Social tipping processes towards climate action: a conceptual framework. Ecol Econ 2022;192:107242.
[6] Wilson KG, Kogut J. The renormalization group and the ϵ expansion. Phys Rep 1974;12:75–199.
[7] de Gennes P. Scaling concepts in polymer physics. Cornell University Press; 1979. Available from: https://books.google.de/books?id=Gh1TcAAACAAJ.
[8] Schadschneider A. Statistical physics of traffic flow models. Physica A 2000;285:101–20.
[9] Helbing D, Lozano S. Phase transitions to cooperation in the prisoner's dilemma. Phys Rev E 2010;81:057102.
[10] Garcia D, Abisheva A, Schweighofer S, Serdült U, Schweitzer F. Ideological and temporal components of network polarization in online political participatory media. Policy Internet 2015;7:46.
[11] Perc M, Jordan JJ, Rand DG, Wang Z, Boccaletti S, Szolnoki A. Statistical physics of human cooperation. Phys Rep 2020;687:1–51.
[12] Baumann F, Lorenz-Speen P, Sokolov IM, Starnini M. Modeling echo chambers and polarization dynamics in social networks. Phys Rev Lett 2020;124:048301.
[13] Baumann F, Lorenz-Speen P, Sokolov IM, Starnini M. Emergence of polarized ideological opinions in multidimensional topic space. Phys Rev X 2021;11:011012.
[14] Moran J, Fosset A, Luzzati D, Bouchaud J-P, Benzaquen M. By force of habit: self-trapping in a dynamical utility landscape. Chaos 2020;30:053123.
[15] Yu Q, Fang D, Zhang X, Jin C, Ren Q. Stochastic evolution dynamics of the rock-scissors-paper game based on a quasi birth and death process. Sci Rep 2016;6:28585.
[16] Wu T, Fu F, Wang L. Coevolutionary dynamics of aspiration and strategy in spatial repeated public goods games. New J Phys 2018;20:063007.
[17] Tomassini M, Antonioni A. Computational behavioral models for public goods games on social networks. Games 2019;10:35.
[18] Burton-Chellew MN, West SA. Payoff-based learning best explains the rate of decline in cooperation across 237 public-goods games; 2021.
[19] Barfuss W. Dynamical systems as a level of cognitive analysis of multi-agent learning. Neural Comput Appl 2022;34:1653–71.
[20] Godara P, Aléman TD, Herminghaus S. Bounded rational agents playing a public goods game. Phys Rev E 2022;105:024114.

[21] Herrmann B, Thöni C, Gächter S. Antisocial punishment across societies. Science 2008;319:1362–7.
[22] Godara P, Herminghaus S. Bounded learning and planning in public goods games. Phys Rev E 2023;107:054140. https://doi.org/10.1103/PhysRevE.107.054140.
[23] Hutter M. A theory of universal artificial intelligence based on algorithmic complexity. Available from: arXiv preprint. arXiv:cs/0004001, 2000.
[24] Ortega DA, Braun PA. Information, utility and bounded rationality; 2011. p. 269–74.
[25] Burton-Chellew MN, Nax HH, West SA. Payoff-based learning explains the decline in cooperation in public goods games. Proc R Soc B 2015;282.
[26] Isaac RM, Walker JM. Group size effects in public goods provision: the voluntary contributions mechanism. Q J Econ 1988;103:179–99.
[27] Pereda M, Capraro V, Sanchez A. Group size effects and critical mass in public goods games. Sci Rep 2019;9:5503.
[28] Bellman R. On the theory of dynamic programming. Proc Natl Acad Sci 1952;38:716–9.
[29] Fudenberg D, Levine DK. Recency, consistent learning, and Nash equilibrium. Proc Natl Acad Sci 2014;111:10826–9.
[30] Ouvrard X. Hypergraphs: an introduction and review. Available from: arXiv preprint. arXiv:2002.05014, 2020.
[31] Bonacich P. Power and centrality: a family of measures. Am J Sociol 1987;92:1170–82.
[32] Benzi M, Klymko C. On the limiting behavior of parameter-dependent network centrality measures. SIAM J Matrix Anal Appl 2015;36:686–706.
[33] Santos FC, Santos MD, Pacheco JM. Social diversity promotes the emergence of cooperation in public goods games. Nature 2008;454:213–6.